Diesel PM Collection for Marine and Automobile Emissions using EHD Electrostatic Precipitators

T. Yamamoto[(1)], T. Mimura[(1)], N. Otsuka[(1)], Y. Ito [(1)], Y. Ehara[(1)], and A. Zukeran[(2)]
[(1)] Department of Electrical and Electronics Engineering, Tokyo City University
1-28-1 Tamatsutsumi Setagaya-ku, Tokyo, 158-8557 Japan
[(2)] Road Systems Engineering Department, Fuji Electric Systems Co. Ltd.
1 Fiji-machi, Hino City, Tokyo, 191-8502, Japan
Yama-t@tcu.ac.jp

***Abstract*—The collection of low resistive particulate matter (PM) generated from marine and automobile engines have been known to be difficult. The collection efficiency for three types of electrostatic precipitators (ESPs) such as conventional DC energized ESP, trapezoidal-waveform energized ESP (TW ESP), and electrohaydrodynamically-enhanced ESP (EHD ESP) were investigated. The EHD ESP utilizes the ionic wind, combined with electrostatic force to transport the charged particles into the pocket effectively attached to the collection plate. The low resistive diesel PMs are detached from the collection plate by the electrostatic repulsion force caused by induction charge, which overcomes the particle adhesion force, resulting in reentrainment. The conventional DC energized ESP showed good collection efficiency for particle size less than 300 nm where adhesion force was dominated over electrostatic repulsion force but showed a severe reentrainment for the particle size greater than 1,000nm, while TW energized ESP suppressed the particle reentrainment for larger particles but still showed negative collection efficiency. On the other hand, the EHD ESP showed an excellent collection efficiency for particle size up to 1,000 nm and significant reentrainment suppression was observed for particle size greater than 2,000 nm.**

Keywords- *Diesel engine, marine engine, EHD, electrostatic precipitator, ionic wind, low resistive dust, reentrainment*

I. INTRODUCTION

The particles emitted from diesel engine exhaust have low resistive in nature and extremely small in the range of 70~120 nanometers (nm). These particles are penetrated into an alveolus and extremely harmful to human health. These particles are generated from various emissions such as diesel automobiles, marine engines, power generation engines, and construction diesel machines. The collection of low resistive particles (PM) generated from marine and automobile engines have been known to be extremely difficult. The low resistive diesel engine particles are detached from the collection plate where the electrostatic repulsion force due to induction charge overcomes adhesion force. This phenomenon was known as particle reentrainment, resulting in poor collection efficiency. The use of diesel particulate filter was widely used for collection of automobile diesel PM but was not economical and cost effective, especially for marine engine emission control.

The regulation for automobile diesel engine particulate matter (PM) emission was set at 0.01 g/kWh and 0.7 g/kWh for NOx by the year 2009. On the other hand, the marine engine regulation was at 0.2~0.4 g/kWh for PM, 7.2~7.4 g/kWh for NOx, and 4 g/kWh for CO in the US and 1.0 g/kWh for PM, 9.8 g/kWh for NOx and 5 g/kWh for CO in Europe and Japan by MARPOL treaty in 2005. More stringent regulations are coming up in the near future.

There are few literatures describing the control of particle reentrainment [1-3]. Recently, two-stage ESP using charging zone by DC field, followed by the collection zone by low frequency AC field in the range of 1 Hz has been developed for the collection of diesel particles in tunnel [4-6], while the conventional ESP utilizes DC high voltage. Several pocket design collection plate were reported but was not taken into account the EHD to transport the charged particles into the pocket zone [7]. Some ESP manufactures use the corrugated collection plates. However, the primary reason was to increase the strength of large plate assembly but this design may help preventing trapping loss in the corrugated section. However, both concepts have limited success for minimizing the reentrainment. The wet ESP was another strong candidate for this application but it creates water treatment as opposed to dry process.

Based on fundamental concept of reentrainment, the new electrohydrodynamically-assisted ESP (EHD ESP) was developed to overcome the reentrainment in the ESP [8]. The EHD ESP, which utilizes the ionic wind to transport the charged particles effectively into the pocket zone attached to the collection plate. The captured particles are trapped in the pocket and the pocket zone was exposed to zero electric field, so that no electrostatic repulsion force by induction charge takes place, which is the major factor for the reduction of particle reentrainment. The effectiveness of the EHD ESP was demonstrated to show the significant suppression of particle reentrainment [8]. However, the engine size was 199cc using light oil, which the maximum gas velocity obtained in the EHD ESP was 0.74 m/s. The EHD ESP was improved to minimize the sneakage of the gas by adding the baffle plates. The investigation was also expanded to include the use of 2.3 L engine using heavy oil (Hokuetsu kogyo, PDS175S) to achieve higher flow velocity.

In the present study, three electrostatic precipitators (ESPs) such as conventional DC energized ESP, trapezoidal-waveform energized ESP (TW ESP), and EHD ESP were .investigated. The particle size-dependent collection efficiency was obtained for three ESP operations using Scanning Mobility Particle Sizer (SMPS TSI, 20-300 nm) and particle counters (RION PC 300-5,000 nm).although ESP sizes were different. The effectiveness of reentrainlent for tree ESPs was compared.

II. EXPERIMENTAL SETUP

Emissions from a small diesel engine generator (Yammer Co., Ltd., YDG200A-5E, direct injection type for a single cylinder, displacement volume of 199cc, maximum electric power output of 1.7 kW) using light oil and the 2.3 L engine using heavy oil A (Hokuetsu Kogyo, PDS175S) with 2,000 rpm were used to achieve a high velocity flow. These diesel engines were connected to the three types of ESPs. The EHD ESP reported earlier [8] was modified to add the buffer plates in the ESP to minimize the sneakage. In this experiment, whole exhaust flue gas was treated. In order to determine the number particle density in the ESP, the flue gas was diluted approximately 1,000 times by ambient air and particle size-dependent number densities before and after the ESPs were determined by the SMPS (Scanning Mobility Particle Sizer, Model 3034) for the particle size ranged 20-800 nm and the particle counter (Rion KC-01C) for the article size of 300-5,000 nm. The exhaust gas temperature was nearly 20°C. The gas velocity was measure by the hot wire anemometer (Kanomax)

The ESPs used for this experiment were shown in Figs. 1 and 2 and their dimensions were designated in the figures. Fig. 1 shows the conventional ESP which consists of plate to plate configuration with shape edges on both sides for charging section using DC, followed by plate to plate collection configuration energized by DC and trapezoidal waveform with two different frequencies (2 Hz with two different voltage modes and 20kHz). The electrode distance was set at 9 mm for both charging and collection plates. All other dimension was shown in Fig. 1. There are 5 gas passages in the ESP.

The EHD ESP consists of five teeth shaped electrode and the collection plate with six pockets. The channel width was 60 mm and its effective height was 200 mm. The pockets with 10 mm depth are attached to the collection plate with every 6 cm interval as shown in Fig. 2. The discharge electrode was the saw type, and their teeth were equally spaced with the interval of 10 mm. The overall dimension of ESP section was 300 mm high and 420 mm wide without hopper and inlet and outlet transitions. The flue gas was connected to inlet and outlet of the ESP through the transition where 50% opening perforated plates were placed to achieve the uniform flow in the ESP. The bottom section of EHD ESP has hopper section with buffer plates, so that particle sneakage was minimized. At the same time the fraction of particle collection can be measured for each electrode section. The top section was made out of plexiglass for visualizing EHD flows and particle transport in the EHD ESP.

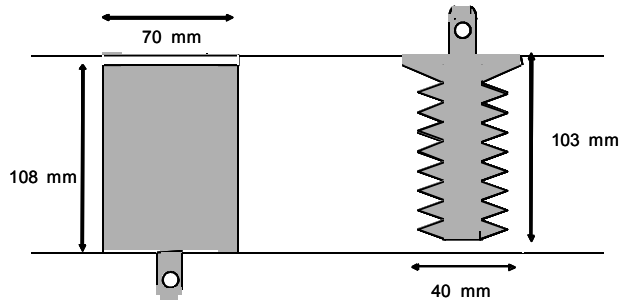

(a) Charging section

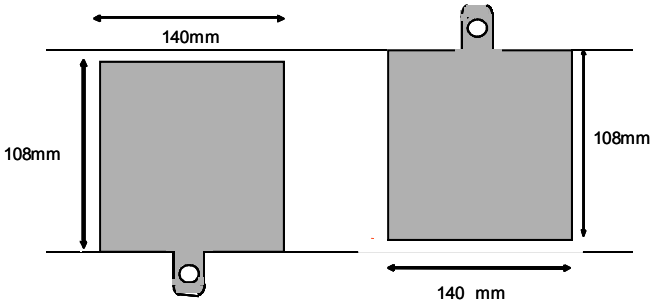

(b) Collection section

Fig. 1. The conventioanl ESP configuration

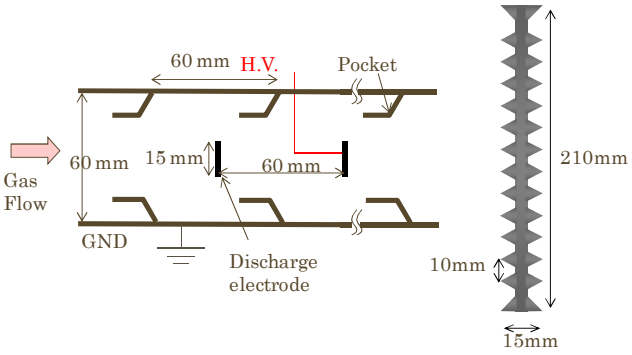

Fig. 2. The EHD assisted ESP configuration

Fig. 3 shows four different waveforms used in the collection plate sections for the conventional ESP configuration as shown in Fig. 1: (1) DC, (2) trapezoidal waveform with 0~-6 kV and frequency of 2 Hz, designated as NT1-0 (average electric field of 6.7 kV/cm), (3) trapezoidal waveform with +2~-6 kV and frequency of 2 Hz, designated as NT1-2, (4) trapezoidal waveform with 0~-6 kV and frequency of 20 Hz, designated as NT0.1-0. On the other hand, EHD ESP used negative polarity energized by DC with modest applied voltage of -10kV (5 kV/cm based on the shortest distance of 2cm) although the spark voltage was 18kV).

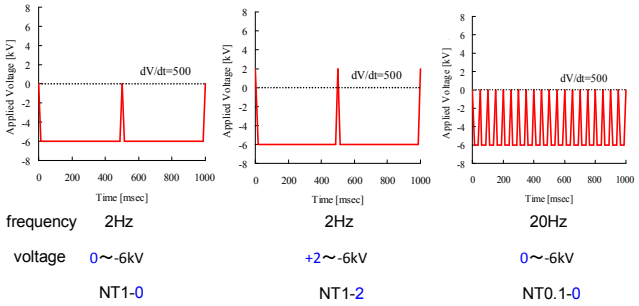

Fig. 3. Trapezoidal waveform with various operation modes

III. RESULTS AND DISCUSSION

3.1 Experimental Results using 199cc Engine with Light Oil

When the engine load was set at 100% (1.7kW) with the gas flow velocity of 0.3 m/s, the particle-size dependent number density in the range of 20~300 nm was evaluated using four different energization methods for the conventional ESP. Fig. 4 shows the particle size dependent number density using SMPS and the corresponding collection efficiency as shown in Fig. 5. The number density was increased with load and was as high as $3x10^{10}$ particles/cm^3 at peak particle size of 100 nm for inlet concentration. The maximum efficiency with more than 90% of collection efficiency was achieved with DC energization, followed by 2Hz trapezoidal waveform designated as NT1-0, NT1-2, and NT0.1-0. The minimum efficiency achieved was about 78% and occurred at 200 nm. This was attributed to lower average field during lower voltage, which corresponds to classical charging theory.

The adhesion force, Fad, was Van der Waals force, expressed as: $Fad = - Hd/12z^2$, where H = Hamaker constant, d = particle diameter, and z = particle separation. Fad consists of adhesion force which depends on the area of contact zone and capillary force when the moisture exists between particle and surface. An empirical adhesion force (dyn or 10^{-5} N) for spherical aluminum oxide particle, 10~50 μ m in diameter to a steel surface give the following equation [9]: $Fad = 2.6d^{-0.7}$ for

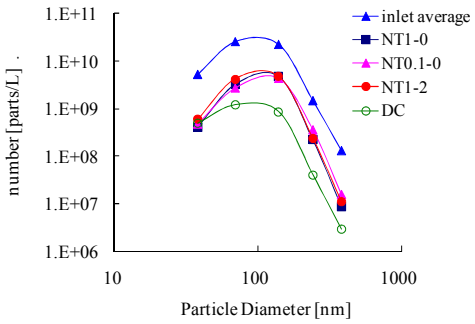

Fig. 4 Particle size-dependent number density with SMPS for various operating modes for the conventional ESP when the gas velocity was 0.3 m/s

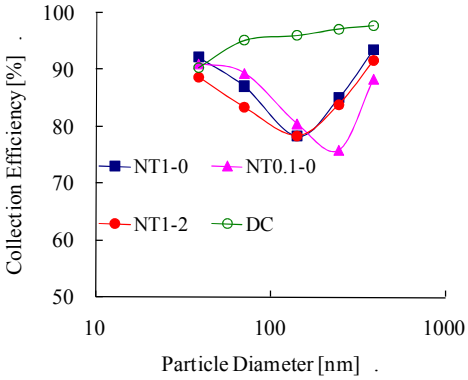

Fig. 5 Particle size-dependent collection efficacy with SMPS for various operating modes for the conventional ESP when the gas velocity was 0.3 m/s

d=10 ～ 50 μ m. The adhesion force dominated over the electrostatic repulsion force due to induction charge for the particle size in the range of 20~300 nm, resulting in no reentrainment takes place for the conventional ESPs.

On the other hand, the number density for particle size of 300~5,000 nm was shown in Fig. 6. The corresponding collection efficiency was shown in Fig. 7. The collection

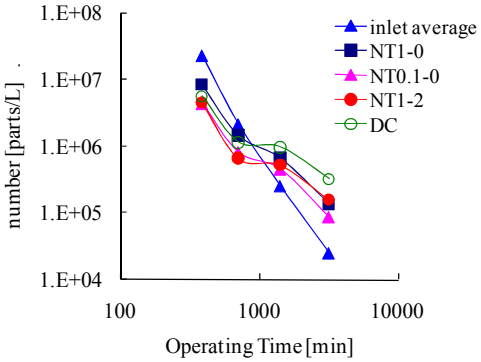

Fig. 6 Particle size-dependent number density with PC for various operating modes for the conventional ESP when the gas velocity was 0.3 m/s

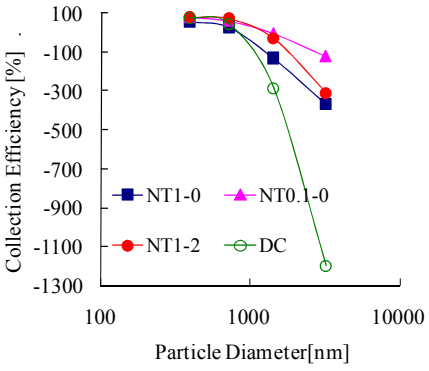

Fig. 7 Particle size-dependent collection efficacy with PC for various operating modes for the conventional ESP with V_o=0.3 m/s

efficiency decreases with increased particle size. The best collection efficiency achieved was the case of NT0.1-0, followed by NT0-2, NT1-0. The worst efficiency was for the case of DC energization, which -1,200% efficiency was obtained. Obviously, it was caused by particle reentrainment due to repulsion force due to induction charge since it is proportional to the square of electric field and particle size. The trapezoidal shape waveform (NT10-0, NT0.1-0, and NT1-2) suppressed the reentrainment but still shows negative collection efficiency even at 0.3 m/s of gas flow velocity. Among trapezoidal waveforms, NT1-2 shows the best performance. The explanation to minimize the particle reentrainment was as follows. Within the ESP, charged particles form dendrite on the collection plate, which are bended back to the collection plate when AC voltage was reversed. This leads to the reduction of aerodynamic drag force exposed to the dendrite formed particles, which results in the reduction of reentrainment [5-7].

Fig. 8 shows the particle size dependent number density for the EHD ESP measured by SMPS. The applied voltage was 12 kV when the load was 60% (1.0 kW) and the gas velocity was 0.37 m/s. The corresponding collection efficiency was greater than 90% up to 800 nm as shown in Fig. 9. The collection efficiency decreased to 80% range above 800 nm. The particle size dependent collection efficiency for particle size in the range of 300-5,000 nm was shown in Figs. 10. The

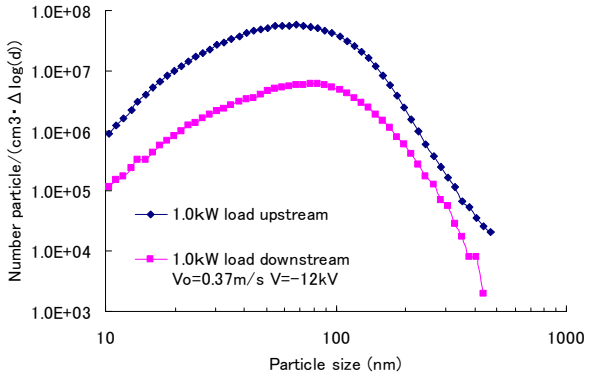

Fig. 8 Particle size-dependent number density uaing SMPS for 60% load with V=12kV and V_o=0.37 m/s for the EHD ESP

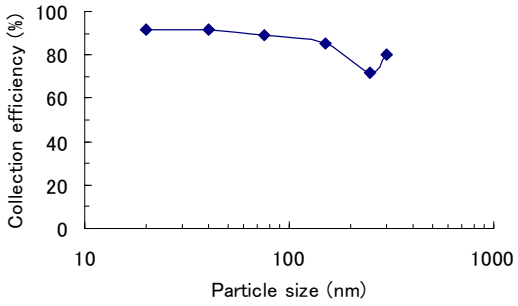

Fig. 9 Particle size-dependent collection efficiency using SMPS for 60% load with V=12 kV and V_o=0.37 m/s for the EHD ESP

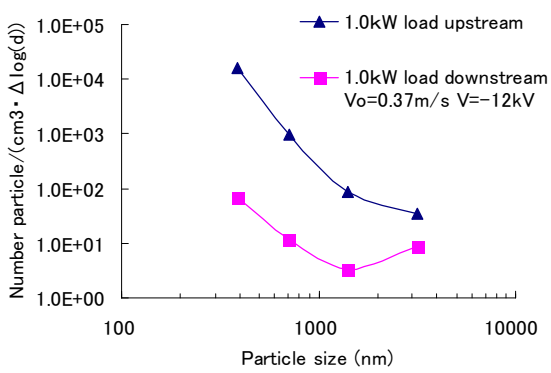

Fig. 10 Particle size-dependent collection efficiency using PC for 60% load with V=12 kV and V_o=0.37 m/s for the EHD ESP

collection efficiency was excellent for 300-1,000 nm but decreased as particle size increased. No negative collection efficiency or particle reentrainment was observed for the EHD ESP, while DC and trapezoidal waved form showed negative collection efficiency.

Fig. 11 shows the time-dependent collection efficiency for the particle size of 300-500 nm, 500-1,000 nm, 1,000-2,000 nm, and 2,000-5,000 nm. The excellent collection was achieved for 300-2,000 nm but decreased to 50-90% for particle size of 3,000-5,000 nm. This fluctuation was due to small number particles for this particle size range. No negative collection efficiency was observed for EHD ESP.

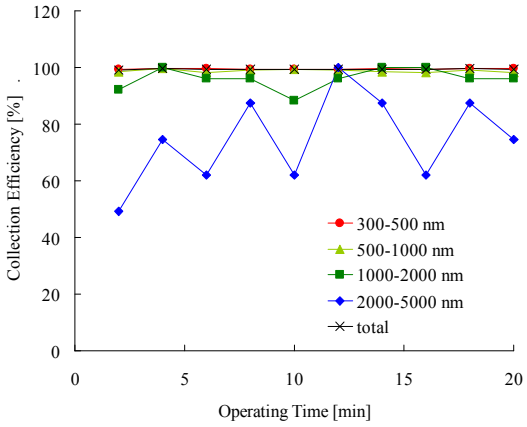

Fig. 11 Time dependent collection efficiency or the particle size range and the overall efficiency using PC for 60% load with V=12 kV and V_o=0.37 m/s for the EHD ESP

3.2 Experimental Results using 2.3L Engine with Heavy Oil A

A 2.3 L diesel engine using A heavy oil was used. The engine was sun at 2,000 rpm and the load was not able to change for this experiments. The gas velocity was increased to 2 m/s using 2.3 L engine. Figs. 12 and 13 show the particle size dependent number density and collection efficiency for the EHD ESP, which was measured by SMPS when the applied voltage was 10 kV. One order of magnitude reduction was achieved for particle size of 300-500 nm. The collection

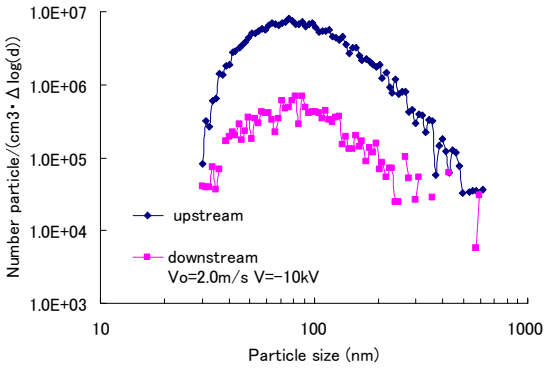

Fig. 12 Particle size-dependent number density uaing SMPS for 2.3 L diesel engine with V=10 kV and V_o=2 m/s for the EHD ESP

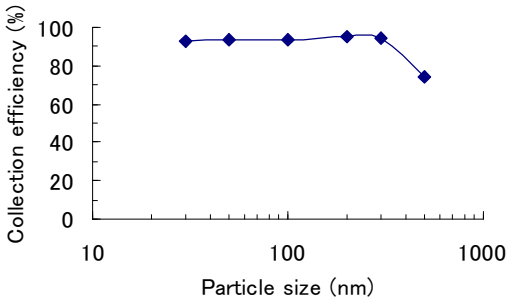

Fig. 13 Particle size-dependent collection effieicy uaing SMPS for 2.3 L diesel engine with V=10 kV and V_o=2 m/s for the EHD ESP

efficiency was decreased beyond 300 nm and reached about 80%.

The particle size-dependent collection efficiency for particle size in the range of 300-5,000 nm was shown in Figs. 14. The collection efficiency was excellent up to 300-1,000 nm but decreased as particle size increased. At particle size of 3,000 nm, the collection efficiency was slightly negative, indicating reentrainment for the EHD ESP. However, number density at 3,000\-5,000 nm was less than 10 so that the fluctuation of efficiency change was significant.

Fig. 15 shows the time-dependent collection efficiency for the particle size of 300-500 nm, 500-1,000 nm, 1,000-2,000 nm, 2,000-5,000 nm, and the overall efficiency when the gas velocity of 2 m/s and applied voltage of 10 kV. The excellent collection was achieved for 300-2,000 nm but decreased to 50-90% for 3,000-5,000 nm. This large fluctuation was again due to small number density in the order of less than 10. Negative collection efficiency indicated that the agglomerated large particles captured at the electrostatic field exposed were detached and reentained by the repulsion force caused by induction charge. In addition, the high flow velocity increased fluid dynamic shear stress, resulting in reentrainment.

The EHD ESP showed significant reduction of reentrainment over the conventional ESPs with different operating modes. However, we are still looking for the

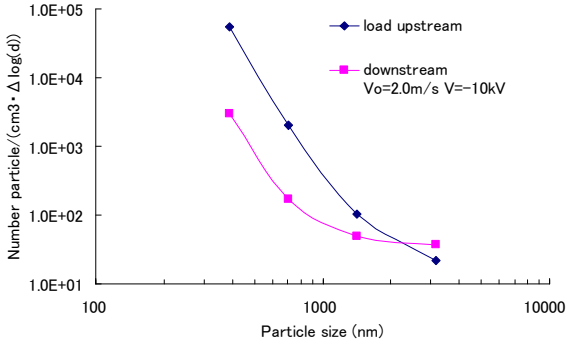

Fig. 14 Particle size-dependent collection effieicy uaing PC for 2.3 L diesel engine with V=10 kV and V_o=2 m/s for the EHD ESP

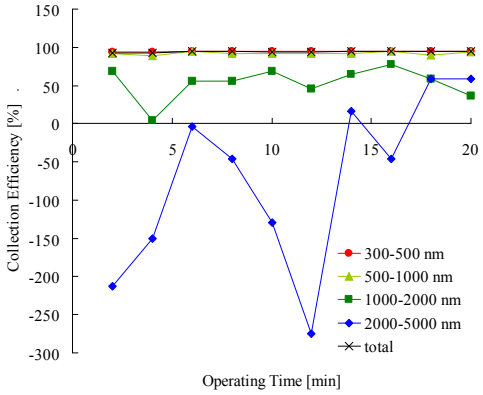

Fig. 15 Time-dependent collection efficiency for the particle size range and the overall efficiency for EHD ESP with V=10 kV and V_o=2 m/s for the EHD ESP

optimum design to minimize the reentrainment for the EHD ESP by transporting the charged particle into the pocket effectively and minimizing the electric field exposed area even the increased gas velocity (in the range of 10 m/s .

IV. SUMMARY

The collection of low resistive particles generated from marine and automobile engines was investigated using two types of ESPs such as conventional DC energized ESP, trapezoidal-waveform energized ESP, and electrohaydrodynamically-enhanced ESP (EHD ESP). The conventional DC energized ESP showed good collection efficiency for particle size less than 300 nm where adhesion force was dominated over electrostatic repulsion force but showed severe reentrainment for the particle size greater than 1,000nm. The trapezoidal waveform energized ESP suppressed the particle reentrainment for larger particles but still showed negative collection efficiency. On the other hand, the EHD ESP demonstrated an excellent collection efficiency for particle size less than 1,000 nm and significant suppression of particle reentrainment was achieved even at high flow velocity, compared with the conventional ESP.

ACKNOWLEDGMENT

Authors wish to thank you for support by Grant-in-Aid for Scientific Research (B) of the Japanese Society for the Promotion of Science.

REFERENCES

[1] "Handbook of Electrostatics" Ed. S. Masuda, Ohm Press, Institute of Electrostatics Japan

[2] J.D. Bassett, K. Akutsu, S. and Masuda, "A Preliminary Study of Re-entrainment in an Electrostatic Precipitator," *Journal of Electrostatics,* Vol. 3, 1977, pp. 311-257.

[3] R. M. Felder, E. Arce-Medina, "Radiotracer Measurement of Local Despsition Profiles, Friction Reentrainment and Impaction Reentrainment in an Electrostatic Precipitator," *AIChE Journal*, Vol. 31, No. 1, 1985, pp. 82-89.

[4] T. Takahashi, Y. Kawada, A. Zukeran, Y. Ehara, and T. Ito, "Inhibitory Effect fo Coating Elctrodes with Dielectric Sheet on Re-entrainment in Electrostatic Precipitator," *Journal of Aerosol Science*, Vol. 29, Suppl. 1, 1998, pp.s481-s82.

[5] A. Zukeran, Y. Ikeda, Y. Ehara, M. Matsuyama, T. Ito, T. Takahashi, H. Kawakami, and T. Takamatsu, "Two-Stage Type Electrostatic Precipitator Re-entrainment Phenomena under Diesel Flue gases," *IEEE Trans. Ind. Applications*, Vol. 35, No. 2, 1999, pp. 346-351.

[6] A. Zukeran, Y. Ikeda, Y. Ehara, T. Ito, T. Takahashi, H. Kawakami, and T. Takamatsu, "Agglomeration of Particles by ac Corona Discharge," *EEJ*, Vol. 130, No. 1, 2000, pp. 30-37.

[7] K. Yasumoto, A. Zukeran, Y. Takagi, Y. Ehara, T. Takahashi, and T. Ito, "Suppression of Particle Deposition onto Downsteram Wall in an AC Electrostatic Precipitator with Neutralization," Int. Journal of Environment and Waste Management, Vol. 2 NOs4/5, 2008, pp.399-411.

[8] T. Yamamoto, T. Abe, T. Mimura, Y. Ito, N. Otsuka, Y. Ehara, and A. Zukeran, "Electrodynamically-Assisted Electrostatic Precipitator for Collection of Low Resisitve Diesel Particulates," Proc. of IEEE-IAS, Edmonton Canada Oct. 5-9,2008, CDROM 6pagers.

[9] A.D. Zimon, Adhesion of Dust and Powder, Plenum Press, New York, London 1969.

[10] T. Yamamoto, and H.R. Velkoff, "Electrohydrodynamics in an Electrostatic Precipitator." *J. of Fluid Mechanics*, Vol. 108, 1981, pp. 1-18.

[11] H.Y. Wen and G. Gasper, "On the Kinetics of Particle Reentrainment from Surface," *J. Aerosol Science*, Vol. 20, 1989, pp. 483-498.

[12] M.W. Reeks, J. Red, and D. Hall,"On the Resuspension of Small Particles by a Turbulent Flow," *J. Physics D, Applied Physics*, Vol. 21, 1988, pp. 574-589.

[13] M.M.R. Williams, "An Exact Solution of the Reek-Hall Resuspension Equation for Particulate Flow," *J. Aerosol Science*, Vol. 23(1), 1992, pp. 1-10.

[14] T. Yamamoto, M. Okuda, and M. Okubo, "Three Dimensional Ionic Wind and Electrohydrodynamics of Tuft/Point Corona Electrostatic Precipitators," *IEEE Transactions on Industry Applications*, Vo. 39, No. 6, Nov/Dec 2003, pp. 1603-1607.

[15] H. Fujishima, Y. Morita, M. Okubo, and T. Yamamoto, "Numerical Simulation of Three-Dimensional Electrohydrodynamics of Spiked-Electrode Electrostatic Precipitators," I*EEE Transactions on Dielectric and Electrical Insulation*, Vo. 13, No. 1, Feb. 2006, pp. 160-167.